Progress In Electromagnetics Research, Vol. 135, 657–675, 2013

HYBRID TECHNIQUE FOR THE ANALYSIS OF SCATTERING FROM PERIODIC STRUCTURES COMPOSED OF IRREGULAR OBJECTS

Adam Kusiek*, Rafal Lech, and Jerzy Mazur

Gdansk University of Technology, 11/12 Narutowicza Street, Gdansk 80-233, Poland

Abstract—In the paper, the analysis of electromagnetic wave scattering from multilayered frequency selective surfaces is presented. The surface is composed of periodically arranged posts with irregular shapes. The multimodal scattering matrix of such structure is derived and the transmission and reflection characteristic for the structure with arbitrary plane wave illumination are calculated. The exact full-wave theory based on the hybrid approach employing mode-matching method and finite-difference frequency-domain (FDFD) technique is applied to develop an efficient theory to analyze such structures. The validity and accuracy of the approach are verified by comparing the results with those obtained from alternative methods and own measurements of manufactured periodic structures.

1. INTRODUCTION

The analysis of plane wave scattering from three dimensional (3D) periodic structures composed of multilayered frequency selective surfaces (FSS) is conducted in this paper. Each FSS is composed of periodic in two directions arrangements of scatterers which can be of irregular shapes. These elements are comparable in size to the operation wavelength and are composed of isotropic and anisotropic materials such as conductors, dielectrics, ferrites or semiconductors.

The multilayered FSSs are utilized as an electromagnetic band structure (EBG) in microwave wavelength range or photonic band structure (PBG) in optical range [1, 2]. Recently, EBGs and PBGs are of great interest due to their extraordinary properties and potential applications e.g., filters, polarizers, substrates for radiating elements,

Received 25 October 2012, Accepted 14 December 2012, Scheduled 7 January 2013

* Corresponding author: Adam Kusiek (adakus@eti.pg.gda.pl).

or optical switches [2–15]. FSSs find also application in polarizers and polarization rotators to change the polarization state of an electromagnetic wave [16, 17]. Through the utilization of these devices the antennas adopted to receive a single linear polarization (vertical or horizontal) are able to work with both polarizations at the same time.

Many numerical techniques have been utilized to investigate band gap structures. The most popular are the cylindrical-harmonic expansion method [18], the finite element method [19], the finite-difference method [20], and Fourier modal method [21]. Here we calculate the scattering parameters of periodic arrangements of metalo-dielectric or ferrite scatterers assuming a plane wave excitation of the structure. In order to obtain the scattering parameters we first calculate the multimodal scattering matrices of each layer (each FSS), utilizing authors' numerical technique [22], and then use cascading formulas to obtain the results for the entire structure. The proposed approach utilizes an efficient numerical technique described in [18, 23, 24], which is based on the transmission matrix (**T**-matrix) method [25] and uses the lattice sums technique [26]. The obtained scattering matrix relates the incident space-harmonics to the scattered, both reflected and transmitted ones. It is expressed in terms of lattice sums characterizing a periodic arrangement of scatterers and the **T**-matrix of periodic unit cell of the structure.

In this paper the investigation of cylindrical unit cells employing posts with regular or irregular geometry is presented and analytical method for regular or hybrid technique for irregular shapes are utilized for the calculation of their **T**-matrices. The obtained results are verified by comparing them with ones obtained from commercial simulator and own measurements of manufactured periodic structures.

2. FORMULATION OF THE PROBLEM

The structure under investigation is presented in Fig. 1. It is composed of a 3D array of uniformly spaced identical sections situated in a free space and illuminated by a harmonic wave with arbitrary direction. The sections are composed of scatterers of height d and are spaced with distances h_x, h_y and h_z along axes of rectangular coordinate system.

The aim of the analysis is to find scattering parameters of the investigated structure with the assumption of arbitrary angle of harmonic wave incidence (θ_{in}, ϕ_{in}). In order to determine these parameters the investigated structure is divided into layers (surfaces for a fixed y) which constitute two dimensional (2D) periodic FSSs. Each layer can be described by a multimodal scattering matrix, which relates the incident space-harmonics to the scattered, both reflected

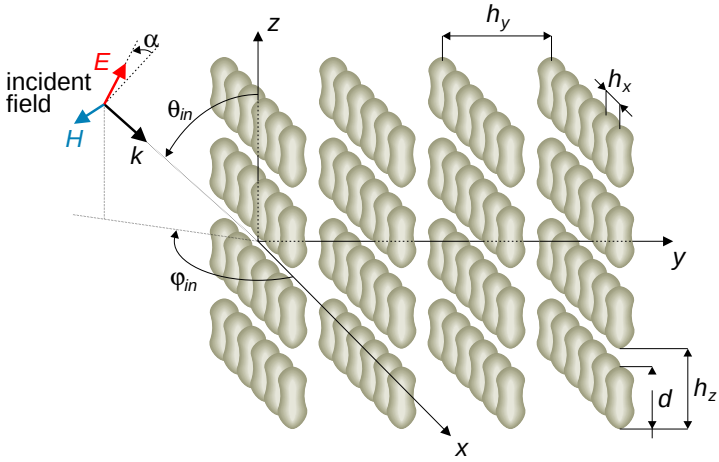

Figure 1. Analyzed periodic configuration.

and transmitted ones, utilizing authors' technique [22] based on an efficient numerical technique described in [18, 23, 24].

Assuming the surface periodic in x and z directions the fields consist of set of space harmonics and the z components of the incident and scattered fields can be described as follows:

$$F_{z,i}^{e(h)} = \sum_p \sum_l a_{1,pl}^{e(h)} e^{j(k_{x,l}x + k_{y,pl}y + k_{z,p}z)} + a_{2,pl}^{e(h)} e^{j(k_{x,l}x - k_{y,pl}y + k_{z,p}z)}, \quad (1)$$

$$F_{z,s}^{e(h)} = \sum_p \sum_l b_{1,pl}^{e(h)} e^{j(k_{x,l}x - k_{y,pl}y + k_{z,p}z)} + b_{2,pl}^{e(h)} e^{j(k_{x,l}x + k_{y,pl}y + k_{z,p}z)}, \quad (2)$$

where $F^e = E$, $F^h = H$, $l = 0, \pm 1, \ldots \pm L$ and $p = 0, \pm 1, \ldots \pm P$ are integers denoting the order of space harmonics, and

$$k_{x,l} = k_{x,0} + \frac{2l\pi}{h_x}, \quad (3)$$

$$k_{z,p} = k_{z,0} + \frac{2p\pi}{h_z}, \quad (4)$$

$$k_{y,pl} = \sqrt{k_0^2 - k_{z,p}^2 - k_{x,l}^2}, \quad (5)$$

where $k_{x,0} = -k_0 \sin\theta_{in} \cos\phi_{in}$, $k_{z,0} = k_0 \cos\theta_{in}$, $a_1^e = \cos\alpha \sin\theta_{in}$, $a_1^h = \sin\alpha \sin\theta_{in}$, and α is an inclination angle of the incoming field on the incidence plane.

The resulting scattering matrix of the periodic surface is defined

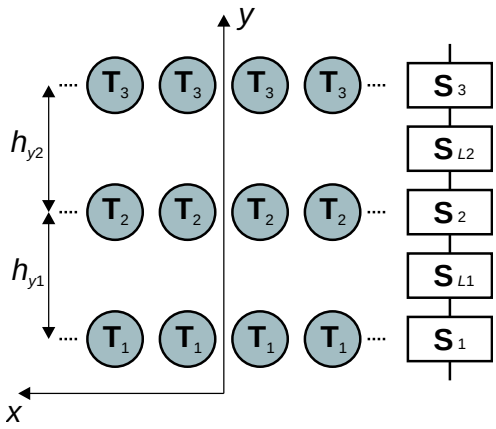

Figure 2. S-parameter representation of multilayered structure.

as follows:

$$\begin{bmatrix} \mathbf{b}_1 \\ \mathbf{b}_2 \end{bmatrix} = \begin{bmatrix} \mathbf{S}_{11} & \mathbf{S}_{12} \\ \mathbf{S}_{21} & \mathbf{S}_{22} \end{bmatrix} \begin{bmatrix} \mathbf{a}_1 \\ \mathbf{a}_2 \end{bmatrix} = \mathbf{S} \begin{bmatrix} \mathbf{a}_1 \\ \mathbf{a}_2 \end{bmatrix}, \tag{6}$$

where $\mathbf{S_{ij}}$ $(i, j = 1, 2)$ are square matrices of $(2 \cdot (2L + 1) \cdot (2P + 1))$ dimensions, and $\mathbf{a_i}$ and $\mathbf{b_i}$ $(i = 1, 2)$ are column vectors of complex amplitudes of $(2 \cdot (2L + 1) \cdot (2P + 1))$ dimension defined as follows:

$$\begin{aligned} \mathbf{a} &= [\mathbf{a}_{-P}, \ldots, \mathbf{a}_P]^T, \\ \mathbf{a}_p &= \left[a^e_{p(-L)}, \ldots, a^e_{pL}, a^h_{p(-L)}, \ldots, a^h_{pL}\right], \end{aligned} \tag{7}$$

where e and h denote TM and TE polarization, respectively, and column vector $\mathbf{b}$ is defined analogously.

Calculating the scattering matrix of one layer it is possible to use cascading formulas to obtain the results for the entire structure, in which layers are spaced with distance h_y along y axis. This approach allows one also to investigate structures composed of layers with different arrangement of scatterers. The schematic representation of multilayered structure is presented in Fig. 2. In this example the structure is composed of three layers each of which is composed of different arrangement and/or size of posts. Each post in the array (unit cell of the periodic array) is represented by its transmission matrix (**T**-matrix), which relates the unknown coefficients of the scattered fields with the known coefficients of the incident fields. The elements of the **T**-matrix are obtained by applying the proper continuity conditions on the surface of scatterer, and depend on the particles size, shape, composition and orientation, but not on the nature of the incident or

scattered fields. As each layer in the structure is different they are described by different scattering matrices ($\mathbf{S}_1$, $\mathbf{S}_2$ and $\mathbf{S}_3$). To use the cascading formula the scattering matrices of the empty spaces between layers of length h_{y1} and h_{y2} need to be considered. The scattering matrix of free space is of identical dimension as the scattering matrices of each layer and is defined utilizing the propagated and decaying space harmonic components as follows:

$$[\mathbf{S_{Li}}] = \begin{bmatrix} [0] & \text{diag}\left(e^{jk_{y,pl}h_{yi}}\right) \\ \text{diag}\left(e^{jk_{y,pl}h_{yi}}\right) & [0] \end{bmatrix} \tag{8}$$

The procedure of calculating scattering matrix of a periodic layer composed of metalo-dielectric posts with regular cross-section is described by authors thoroughly in [22]. It involves the calculation of isolated **T**-matrix of single scatterer in the array, which in the case of objects with simple geometry is carried out with the use of analytical methods. The introduction of more complex objects imposes the application of more universal methods, such as discrete ones. The obtained solution is then utilized in the procedure of obtaining scattering matrix.

To avoid the repetition of the whole approach, presented in [22], in the following chapters only the procedure of calculating **T**-matrix of an isolated scatterer with irregular shape is described.

2.1. T-matrix of an Isolated Scatterer

Consider a single cylinder containing irregular objects arranged periodically along its axis. Each object in the cylinder corresponds to a unit cell of the periodic arrangement. These posts can be of irregular

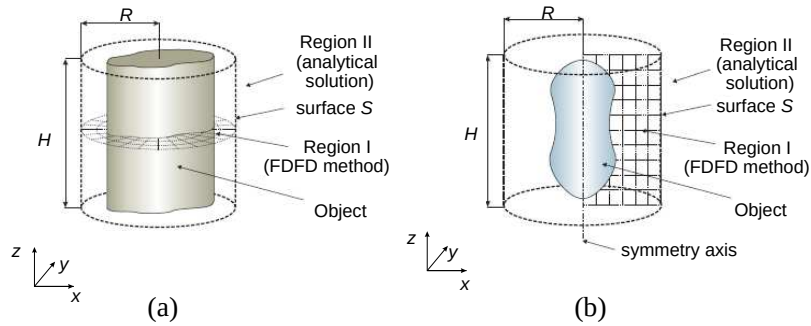

Figure 3. Single unit cell of periodic along z-axis cylinder containing. (a) Cylinder with arbitrary cross-section. (b) Rotationally symmetrical post with irregular shape.

cross-section (see Fig. 3(a)) or have rotational symmetry with irregular shape (see Fig. 3(b)). In our approach we introduce lateral surface $\mathcal{S}$ which surrounds analyzed object and divides the computation domain into two regions I and II. In region I the discrete FDFD solutions of Maxwell equations are used, while in region II we utilize analytical solutions. The z components of electric and magnetic fields in region II are expressed as follows:

$$E_z^{II} = \sum_p \sum_m \left(\hat{a}_{1,pm}^e J_m(k_{\rho,p}\rho) + \hat{a}_{2,pm}^e H_m^{(1)}(k_{\rho,p}\rho) \right) e^{j(m\varphi + k_{z,p}z)}, \quad (9)$$

$$H_z^{II} = \sum_p \sum_m \left(\hat{\hat{a}}_{1,pm}^h J_m(k_{\rho,p}\rho) + \hat{\hat{a}}_{2,pm}^h H_m^{(1)}(k_{\rho,p}\rho) \right) e^{j(m\varphi + k_{z,p}z)}, \quad (10)$$

where $\hat{\hat{a}} = \frac{j}{\eta_0} a$, $\eta_0 = \sqrt{\mu_0/\varepsilon_0}$, $k_{z,p} = k_0 \cos(\theta_0) + \frac{2p\pi}{h_z}$, $k_0 = \frac{2\pi f}{c}$, $J_m(\cdot)$ and $H_m^{(1)}(\cdot)$ are Bessel and first kind Hankel functions, respectively, of m-th order, and $\hat{a}_{1,pm}^{e(h)}$ and $\hat{a}_{2,pm}^{e(h)}$ are incident and scattered field expansion coefficients, respectively, for e-TM, h-TE. The φ field components can be derived from Maxwell equations using (9) and (10) [27]. In region I the tangential components of electric and magnetic fields are defined as follows:

$$E_{z,\varphi}^I(R,\varphi,z) = \sum_{p=-P}^{P} \sum_{m=-M}^{M} c_{pm}^{E_{z,\varphi}} e^{j(m\varphi + k_{z,p}z)}, \quad (11)$$

$$H_{z,\varphi}^I(R,\varphi,z) = \sum_{p=-P}^{P} \sum_{m=-M}^{M} d_{pm}^{H_{z,\varphi}} e^{j(m\varphi + k_{z,p}z)}. \quad (12)$$

Imposing the continuity conditions between tangential components φ and z of electric and magnetic fields on the surface $\mathcal{S}$ and utilizing the orthogonality properties of $e^{j(m\varphi + k_{z,p}z)}$ function over $\varphi \in [0, 2\pi]$ and $z \in [0, H]$ we obtain the following set of matrix equations:

$$\mathbf{M}_{a1}^E \hat{\mathbf{a}}_1 + \mathbf{M}_{a2}^E \hat{\mathbf{a}}_2 = \mathbf{c}, \quad (13)$$

$$\mathbf{M}_{a1}^H \hat{\mathbf{a}}_1 + \mathbf{M}_{a2}^H \hat{\mathbf{a}}_2 = \mathbf{d}. \quad (14)$$

For the sake of brevity all the matrices in Equations (13) and (14) are defined in Appendix A. Now we introduce impedance matrix $\mathbf{Z}$ defined as:

$$\mathbf{c} = \mathbf{Z}\mathbf{d}, \quad (15)$$

which relates the expansion coefficients $\mathbf{c}$ and $\mathbf{d}$ of electric (11) and magnetic (12) fields, respectively. For objects with regular geometry the impedance matrix can be determined utilizing analytical

techniques [22]. However, in the case of objects with irregular shape we utilize finite difference-frequency domain (FDFD) technique [28–30] which will be described in the next section. Since, the **Z**-matrix is known it can be utilized to determine the transmission matrix **T** of the object:

$$\hat{\mathbf{a}}_2 = \mathbf{T}\hat{\mathbf{a}}_1, \tag{16}$$

which defines the relation between incident and scattered field expansion coefficients and is expressed as follows:

$$\mathbf{T} = \left(\mathbf{Z}\mathbf{M}_{a2}^{H} - \mathbf{M}_{a2}^{E}\right)^{-1}\left(\mathbf{M}_{a1}^{E}\mathbf{a}_1 - \mathbf{Z}\mathbf{M}_{a1}^{H}\right). \tag{17}$$

Utilizing approach presented in [22] the **T**-matrix of single object can be used to determine the scattering parameters of structure composed of periodically spaced in the x and z directions scatterers.

2.2. Z-matrix of the Post Using FDFD Method

In our approach we focus on two groups of objects which are homogenous cylinders with arbitrary cross-section (see Fig. 3(a)) and axially-symmetrical posts with irregular shape (see Fig. 3(b)). The analyzed objects can be made of dielectric, metal or gyromagnetic material (ferrite, semiconductor, graphene). Utilizing symmetry properties of investigated posts the analytical variation of field in the z or φ direction can be assumed for the posts from Fig. 3(a) and Fig. 3(b), respectively. This allows to reduce the three dimensional (3D) problem to two-and-a-half (2.5D) one. In the case of post from Fig. 3(a) the variation of field along z-axis is assumed as $e^{jk_{z,p}z}$ and region I is discretized only in z-const plane [29]. On the other hand, when the post from Fig. 3(b) is analyzed, due to its rotational symmetry the variation of the field along φ-axis is assumed as $e^{jm\varphi}$ and region I is disretized only in φ-const plane [30]. To include periodicity of the structure along z-axis the probes of field at $z = H$ are phase shifted by $e^{jk_0\cos(\theta_0)H}$ with respect to field probes at $z = 0$. According to the above assumptions Maxwell equations written in a discrete form are as follows:

$$\mathbf{P}_1\mathbf{D}_1(\mathbf{Q}\mathbf{E} + \mathbf{Q}_b\mathbf{E}_b) = j\omega\mu_0\boldsymbol{\mu}_r\mathbf{S}_1\mathbf{H}, \tag{18}$$

$$\mathbf{P}_2\mathbf{D}_2\mathbf{H} = j\omega\varepsilon_0\boldsymbol{\varepsilon}_r\mathbf{S}_2\mathbf{E}, \tag{19}$$

where $\mathbf{P}_{1,2}$ are matrices of derivatives, $\mathbf{Q}, \mathbf{Q}_b$ are matrices of projection, $\mathbf{D}_{1,2}, \mathbf{S}_{1,2}$ are matrices of space disrcetization, $\mathbf{E}, \mathbf{H}$ are vector of electric and magnetic field probes, respectively, in the inner area of region I and $\mathbf{E}_b$ are the probes of electric field on the surface $\mathcal{S}$ defined

by (11) and (12). After simple algebraic manipulation of (18) and (19) we obtain the relation for $\mathbf{H}$ with respect to $\mathbf{E}_b$ which takes the form:

$$\mathbf{H} = -j\omega\varepsilon_0(\mathbf{G})^{-1}\mathbf{S}^{-1}\mathbf{P}_1\mathbf{D}_1\mathbf{Q}_b\mathbf{E}_b, \tag{20}$$

where $\mathbf{G} = \boldsymbol{\mu}_r{}^{-1}\mathbf{S}_1^{-1}\mathbf{P}_1\mathbf{D}_1\mathbf{Q}\boldsymbol{\varepsilon}_r{}^{-1}\mathbf{S_2}^{-1}\mathbf{P}_2\mathbf{D}_2 + \omega^2\mu_0\varepsilon_0\mathbf{I}$. Using the orthogonality of $e^{j(m\varphi+k_{z,p}z)}$ function and taking each term of (11) as a boundary condition with arbitrary values of $c_{pm}^{E_{z,\varphi}}$, separately the unknown coefficients of magnetic field components expressed on the surface $\mathcal{S}$ as:

$$H_{z,\varphi}^{pm}(\rho = R, \varphi) = \sum_{k=-P}^{P}\sum_{l=-M}^{M} d_{klpm}^{H_{z,\varphi}^{(p,m)}} e^{j(l\varphi+k_{z,k}z)} \tag{21}$$

are determined. Now, utilizing coefficients $c_{pm}^{E_{z,\varphi}}$ and $d_{klpm}^{H_{z,\varphi}}$ the $\mathbf{Z}$ can be obtained as follows:

$$\mathbf{Z} = (\mathbf{D}^{\mathbf{H}})^{-1}\mathbf{C}^{\mathbf{E}}, \tag{22}$$

where $\mathbf{C}^E$ is diagonal matrix, and $\mathbf{D}^H$ is full matrix containing electric and magnetic field expansion coefficients, respectively.

3. ACCURACY OF THE METHOD

In order to perform the calculation of the structure scattering matrix the sums introduced in previous chapter need to be properly truncated. To check the convergence of the presented approach two numerical

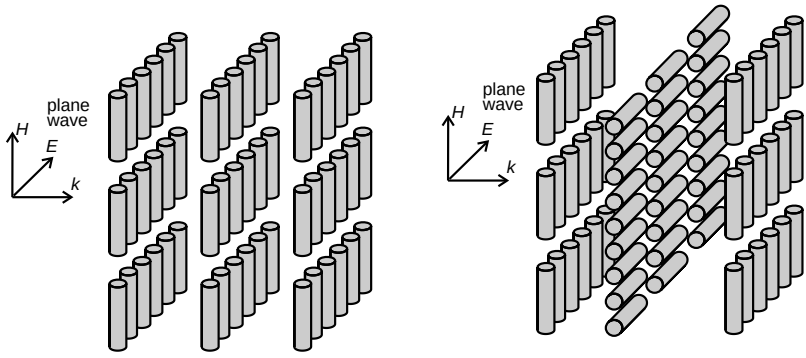

(a) (b)

Figure 4. Schematic representation of triple layer structures composed of periodic cylinders.

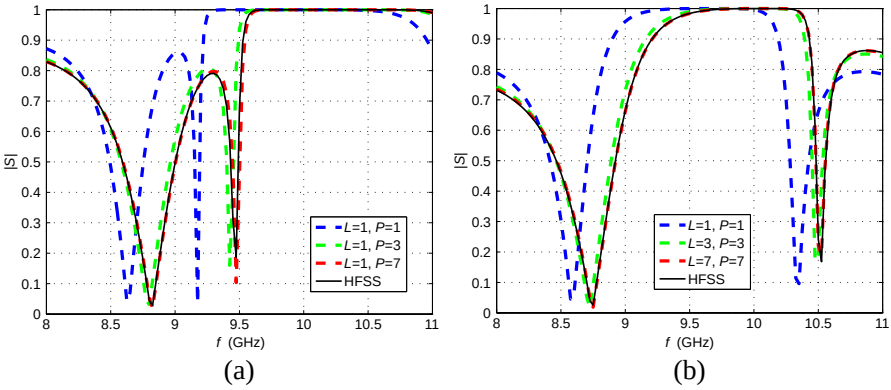

Figure 5. Convergence of reflection coefficients for periodic structures composed of metallic cylinders with circular cross-section of radii $r = 2.5\,\text{mm}$ and height $d = 12\,\text{mm}$ arranged with period $h_x = h_z = 24\,\text{mm}$ and $h_y = 20\,\text{mm}$ for normal incidence. (a) Structure form Fig. 4(a). (b) Structure form Fig. 4(b).

examples depicted in Fig. 4 are considered. Both structures are composed of three layers of metallic cylinders with circular cross-section of radii $r = 2.5\,\text{mm}$ and height $d = 12\,\text{mm}$ arranged with period $h_x = h_z = 24\,\text{mm}$ and $h_y = 20\,\text{mm}$. In the first structure all layers are parallel to each other as illustrated in Fig. 4(a), while in the second structure the middle layer is rotated by 90° with respect to other layers as depicted in Fig. 4(b). The structures are illuminated by a plane wave with $\phi = 90°$, and $\theta = 90°$.

In the analysis the number of cylindrical eigenfunction $M = 7$ was assumed, which provides satisfactory convergence. The convergence of the solution was investigated by changing the number of space harmonics L and P. For the sake of brevity only the convergence of reflection coefficient ($S_{11}^{TM(TM)}$) for both structures is investigated as for other coefficients similar results were obtained. The frequency dependent scattering parameters characteristics of this structure for different values of eigenfunction numbers P and L are presented in Fig. 5.

In order to more accurately examine the convergence of the solution the following error criterion is defined:

$$\delta_S = \frac{||S - S^{ref}||}{||S^{ref}||} \cdot 100\%, \qquad \text{where:} \quad ||\cdot|| = \sqrt{\int_{f_{\min}}^{f_{\max}} |\cdot|^2 df}, \tag{23}$$

Table 1. Convergence of reflection coefficients $S_{11}^{TE(TE)}$, defined by error coefficient δ_S versus eigenfunctions numbers P and L for structure 1 from Fig. 5(a) and structure 2 from Fig. 5(b).

L, P	0,0	1,1	1,2	1,3	1,4	1,5	1,6	1,7	1,8
$\delta_S^{struct\cdot 1}$ [%]	82.77	16.04	8.95	3.68	4.84	0.52	3.50	0.99	0.98
L, P	0,0	1,1	2,2	3,3	4,4	5,5	6,6	7,7	8,8
$\delta_S^{struct\cdot 2}$ [%]	80.13	20.32	8.37	3.87	3.29	1.04	2.25	0.36	0.38

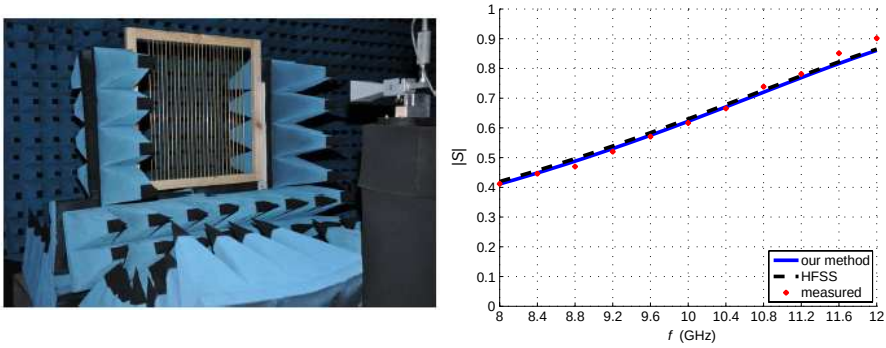

Figure 6. Transmission coefficients for normal plane wave incidence on periodic structures composed of long metallic cylinders with circular cross-section of radii $r = 3\,\text{mm}$ arranged with period $h_x = 20\,\text{mm}$. (a) Picture of manufactured structure. (b) Numerical and measured results.

where S^{ref} are scattering parameters obtained from HFSS based on Finite Element Method (FEM) in frequency domain with periodic boundary conditions. The results are collected in Table 1 and show that the accuracy of the method is improved with the increase of P and L. It can be seen that a sufficient convergence with less then 1% error is obtained for $P = L = 7$ for the second structure while for the first configuration it was sufficient to assume $L = 1$ for the analysis.

Assuming the number of eigenfunctions $P = L = 7$ and $M = 7$, the calculation of single frequency point takes approximately 2.5 s on a Matlab, Xeon X5690 3.47 GHz (2 processors). Comparing this to the calculation of commercial software ANSYS HFSS the time of single frequency point calculation is 118 s with the number of mesh cells 80238. Despite the undeniable fact of high versatility of commercial software a high speed of the proposed method makes it ideal for use in

optimization procedures.

4. RESULTS

Several examples of single and multilayered periodic structures have been investigated. The scattering characteristics of these arrays have been calculated and for the selected arrangements the structures have been manufactured and measured to verify the results. The results are shown for the case of normal incidence as well as for arbitrary angle of incidence. The characteristics are illustrated for refection and

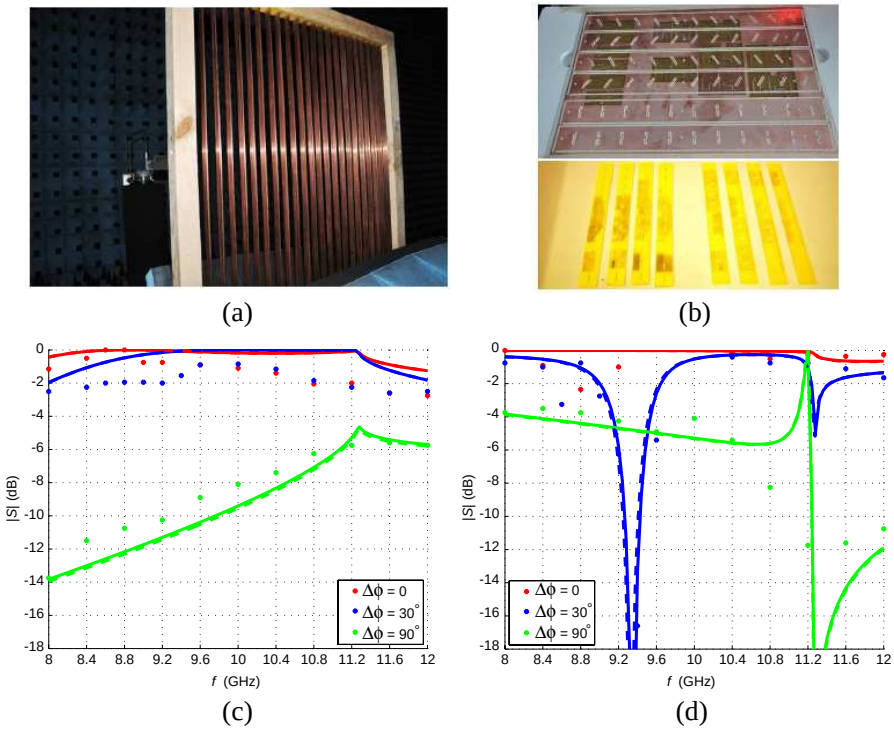

Figure 7. Transmission coefficients for normal plane wave incidence on periodic structures composed of long metallic cylinders with rectangular cross-section with dimensions 15×3 mm arranged with period $h_x = 26.6$ mm for several angles of posts rotation in the array (solid line — our method, dashed line — HFSS, $\times$ — measurements). (a) Picture of manufactured structure. (b) Posts holders in manufacturing process. (c) Numerical and measured results for TM polarization. (d) Numerical and measured results for TE polarization.

transmission coefficients of the fundamental space harmonics ($p = 0$; $l = 0$) versus frequency. For the calculations of the presented examples the maximum number of space harmonics $L = 7$, $P = 7$ and number of cylindrical functions $M = 7$ were chosen which was sufficient to obtain convergence of the solution.

In the first example, the single array of infinitely long metallic cylinders of radii $r = 3\,\text{mm}$ arranged periodically with period $h_x = 20\,\text{mm}$ was considered. The investigated array was manufactured using 60 cm long copper cylinders placed in $60 \times 60\,\text{cm}$ wooden frame as was shown in Fig. 6(a). The grid was measured in anechoic chamber by placing it between two tube antennas with 70 cm distance between the grid and antenna apertures. With this arrangement the measurements of transmission coefficients were performed. The obtained results are shown in Fig. 6(b). As can be observed the measurement results well agree with calculated ones which confirms the correctness of the measurement setup.

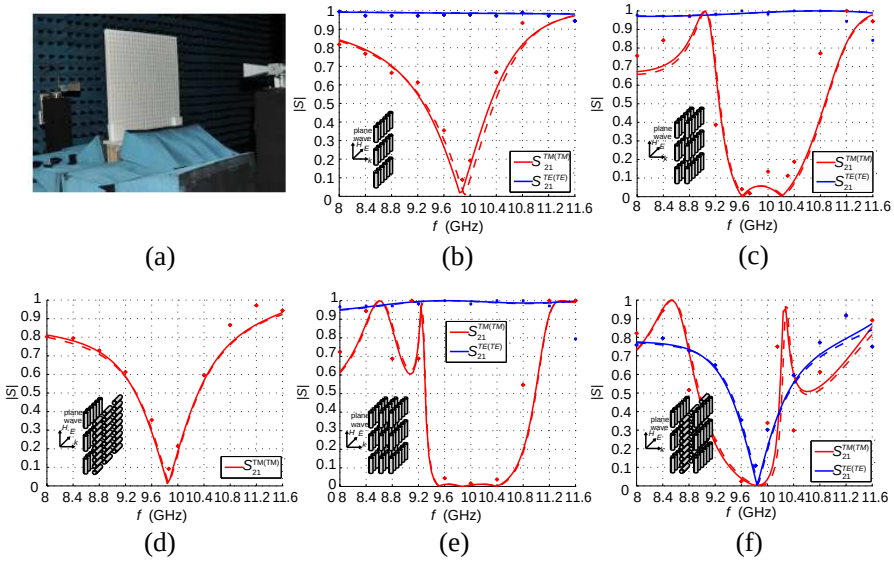

Figure 8. Transmission coefficients for normal plane wave incidence on periodic structures composed of metallic cylinders with circular cross-section of radii $r = 2.5\,\text{mm}$ and height $d = 12\,\text{mm}$ arranged with period $h_x = h_z = 24\,\text{mm}$ and $h_y = 20\,\text{mm}$ (solid line — our method, dashed line — HFSS, $\times$ — measurements). (a) Picture of manufactured periodic arrangement and results for (b) single layer, (c) double layer, (d) double cross layer, (e) triple layer, (f) triple cross layer.

In the second example, the copper cylinders were replaced by copper posts with rectangular cross-section with dimensions 15×3 mm as shown in Fig. 7(a). The structure was measured for different angles of post rotation in the array. In order to set the correct post rotation angle the posts were placed in a special holder (see Fig. 7(b)) which allowed to set both angle and distance between them. The calculated and measured transmission coefficient are shown in Fig. 7(c) for TM polarization and in Fig. 7(d) for TE polarization. As can be observed the satisfactory agreement was obtained.

In another example, single, double and triple layer periodic structures were investigated. The layers were composed of metallic

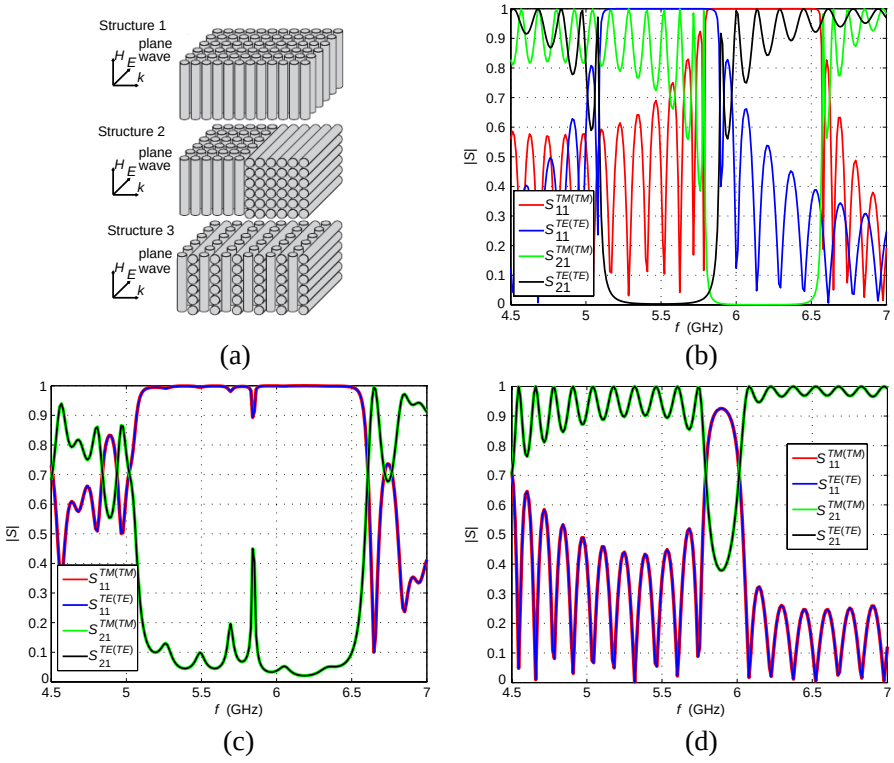

Figure 9. Scattering coefficients for periodic structures composed of 30 layers of infinitely long metallic cylinders with circular cross-section of radii $r = 1$ mm embedded in dielectric cylinders of radii $r = 4.5$ mm with $\varepsilon_r = 6$, arranged with Period $h_x = 22$ mm and $h_y = 25$ mm for normal incidence. (a) Schematic representation of investigated structures. The structures are arranged as (b) structure 1, (c) structure 2, (d) structure 3.

cylinders of radii $r = 2.5\,\text{mm}$ and height $d = 12\,\text{mm}$ arranged with period $h_x = h_z = 24\,\text{mm}$ and $h_y = 20\,\text{mm}$. In order to measure these double periodic layers the posts were placed in $60 \times 60 \times 2\,\text{cm}$ foam made from Rohacell 31 HF material with $\varepsilon_r = 1.05$ (see Fig. 8(a)).

The calculated and measured results for different arrangements of layers are presented in Figs. 8(b)–(f). As can be seen a satisfactory results were obtained between the calculations and measurements.

When a periodic surface is multilayered it constitutes a 3D electromagnetic band gap structure. In a layered system, the multiple interactions of space harmonics scattered from each of the surface layers modify the frequency response, and bandgaps or stop bands in which any electromagnetic wave propagation is forbidden are formed.

The next two examples consider periodic structures composed of

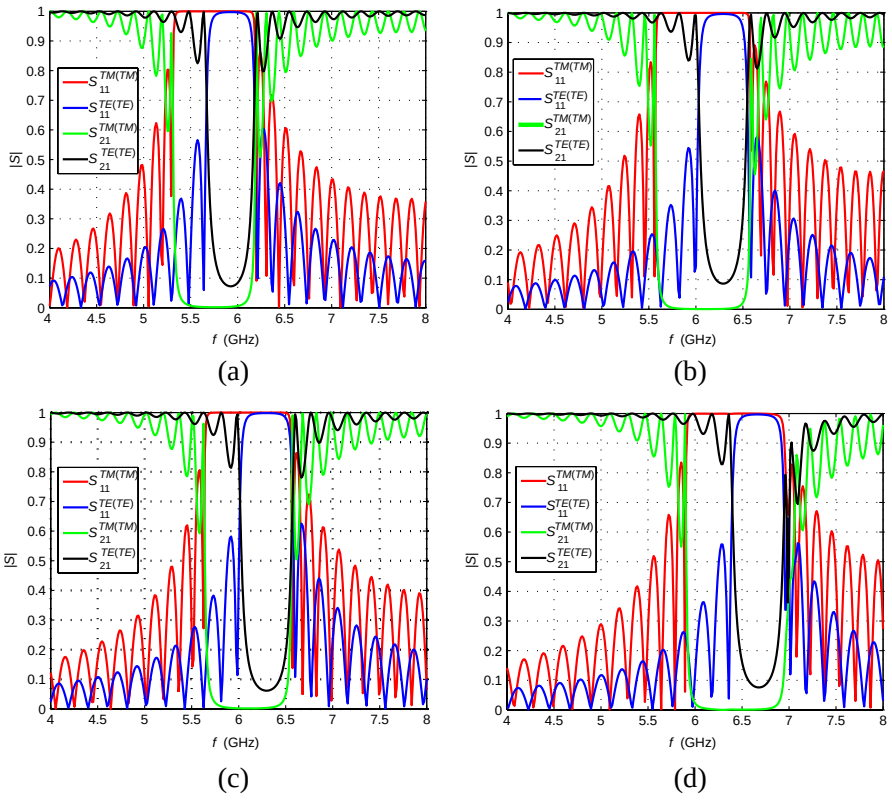

Figure 10. Scattering coefficients for 30-layered periodic structures composed of metallic cylinders with circular cross-section of radii $r = 3\,\text{mm}$ and height $\delta = 10\,\text{mm}$ arranged with period $h_x = h_z = h_y = 25\,\text{mm}$ for (a) normal incidence, (b) $\phi = 70°$, $\theta = 90°$ incidence, (c) $\phi = 90°$, $\theta = 70°$ incidence and (d) $\phi = 70°$, $\theta = 70°$ incidence.

30 layers of single and double periodic surfaces. A single periodic surface is composed of infinitely long metallic cylinders of radii $r = 1\,\text{mm}$ embedded in dielectric cylinders of radii $r = 4.5\,\text{mm}$ with $\varepsilon_r = 6$, arranged with period $h_x = 22\,\text{mm}$. The scattering coefficients calculated for 30 layer structures with different arrangement of layers are presented in Fig. 9. In the first arrangement all the layers are perpendicular as depicted in schematic representation in Fig. 9(a) (structure 1). In the second arrangement first 15 perpendicular layers are followed by identical arrangement rotated by 90° with respect to previous one (structure 2). In the third arrangement every other layer is rotated by 90° (structure 3). As can be observed from the obtained results the first arrangement produces stopbands for both polarizations of the incident plane wave, which only slightly overlap near 5.8 GHz. Using the second arrangement the stopband for both polarizations is widened and covers both stopbands from first arrangement. In the last case the signal with both polarizations can pass through the structure except near 5.8 GHz where both stopbands for first arrangement overlap.

In the next example, the double periodic layer is composed of metallic cylinders with circular cross-section of radii $r = 3\,\text{mm}$ and height $\delta = 10\,\text{mm}$ arranged with period $h_x = h_z = h_y = 25\,\text{mm}$. In this case the structure is illuminated by a plane wave with different

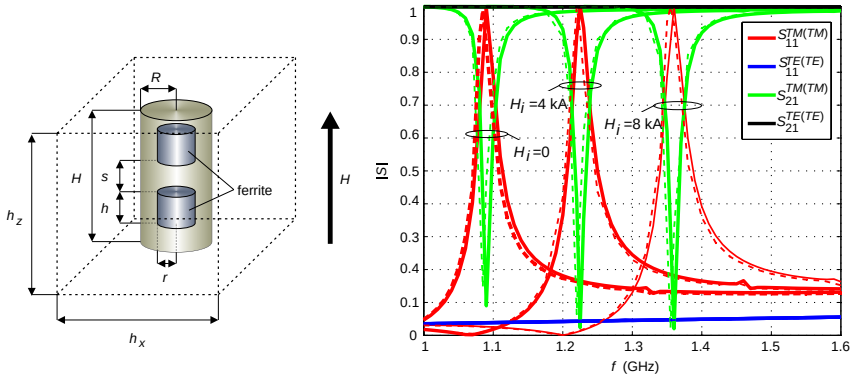

Figure 11. Scattering coefficients for periodic structure ($h_x = h_z = 50\,\text{mm}$) composed of dielectric cylinder ($R = 7\,\text{mm}$, $H = 40\,\text{mm}$, $\varepsilon_r = 3$) loaded with two symmetrically placed ferrite cylinders ($r = 5\,\text{mm}$, $h = s = 10\,\text{mm}$, $\varepsilon_r = 3$). (a) Schematic representation of investigated structure. (b) Scattering parameters for saturation magnetization $4\pi M_s = \{1100\}$ (Gauss) and for different values of internal bias magnetic field intensity $H_i = \{0, 4, 8\}$ (kA) — solid line: our method, dashed line: HFSS.

angles of incidence. The results of this investigation are presented in Fig. 10. For the normal incidence the structure produces stopbands for both polarization in the observed frequency range. Illuminating the structure with different angle it is possible to shift the stopbands and adjust them to the desired frequency.

In the last example, a periodic surface employing dielectric cylinders with double ferrite inclusions (see Fig. 11(a)) is being investigated. The transmission and reflection coefficients for the case of normal plane wave incidence were calculated for different values of internal bias magnetic field intensity $H_i = \{0, 4, 8\}$ (kA) and the results are presented in Fig. 11(b). As can be observed in this case by changing the values of biasing magnetic field it is possible to tune the resonance frequency of the structure, thus to control its frequency response without changing the dimension or arrangement of the structure.

5. CONCLUSION

The analysis of electromagnetic wave scattering from 3D periodic structures has been presented in this paper. The multimodal scattering matrix of such structure is derived using the efficient numerical model based on the transmission matrix approach and lattice sums technique. The transmission and reflection characteristic for the structure with arbitrary plane wave illumination were calculated for several presented examples. The validity and accuracy of the approach were verified by comparing the results with those obtained from alternative methods and own measurements of manufactured structures.

ACKNOWLEDGMENT

This work was supported by the Polish Ministry of Science and Higher Education (National Science Center) from sources for science in the years 2011–2013 under Contract N515 501740 (decision No. 5017/B/T02/2011/40), Contract IP2011 028271 (decision No. 0282/IP3/2011/71) and under funding for Statutory Activities for ETI Gdansk University of Technology.

APPENDIX A.

In Equations (13) and (14) matrices $\mathbf{M}_{a1}^{E(H)}$ and $\mathbf{M}_{a2}^{E(H)}$ take a general form:

$$\mathbf{M}_{\alpha}^{E(H)} = \mathrm{diag}\left[\mathbf{M}_{\alpha,-M}^{E(H)}, \ldots, \mathbf{M}_{\alpha,M}^{E(H)}\right],$$

where $\alpha = \{a_1, a_2\}$,

$$\mathbf{M}^{E}_{\alpha,m} = \begin{bmatrix} \mathbf{M}^{E^e_z}_{\alpha,m} & \mathbf{0} \\ \mathbf{M}^{E^e_\varphi}_{\alpha,m} & \mathbf{M}^{E^h_\varphi}_{\alpha,m} \end{bmatrix}, \quad \mathbf{M}^{H}_{\alpha,m} = \begin{bmatrix} \mathbf{M}^{H^e_\varphi}_{\alpha,m} & \mathbf{M}^{H^h_\varphi}_{\alpha,m} \\ \mathbf{0} & \mathbf{M}^{H^h_z}_{\alpha,m} \end{bmatrix},$$

matrices of electric and magnetic fields take form:

$$\begin{aligned}
[\mathbf{M}^{E^e_z}_{\alpha,m}]_{pp} &= Z_m(k_{\rho,p}R), \quad [\mathbf{M}^{H^h_z}_{\alpha,m}]_{pp} = j/\eta_0 Z_m(k_{\rho,p}R), \\
[\mathbf{M}^{E^e_\varphi}_{\alpha,m}]_{pp} &= \frac{jm}{k^2_{\rho,p}R} Z_m(k_{\rho,p}R), \quad [\mathbf{M}^{E^h_\varphi}_{\alpha,m}]_{pp} = \frac{-\omega\mu_0}{\eta_0 k_{\rho,p}} Z'_m(k_{\rho,p}R), \\
[\mathbf{M}^{H^e_\varphi}_{\alpha,m}]_{pp} &= \frac{-j\omega\varepsilon_0}{k_{\rho,p}} Z'_m(k_{\rho,p}R), \quad [\mathbf{M}^{H^h_\varphi}_{\alpha,m}]_{pp} = \frac{-m}{\eta_0 k^2_{\rho,p}R} Z_m(k_{\rho,p}R)
\end{aligned}$$

and

$$Z_m = \begin{cases} J_m & \text{for} \quad \alpha = a_1, \\ H^{(1)}_m & \text{for} \quad \alpha = a_2. \end{cases} \tag{A1}$$

REFERENCES

1. Yasumoto, K., *Electromagnetic Theory and Applications for Photonic Crystals,* Taylor and Francis, New York, 2006.
2. Jandieri, V., K. Yasumoto, and Y.-K. Cho, "Rigorous analysis of electromagnetic scattering by cylindrical EBG structures," *Progress In Electromagnetics Research*, Vol. 121, 317–342, 2011.
3. Wu, T. K., *Frequency Selective Surfaces and Grid Array,* Wiley, New York, 1995.
4. Munk, B. A., *Frequency Selective Surfaces, Theory and Design* Wiley, New York, 2000.
5. Khromova, I., I. Ederra, R. Gonzalo, and B. P. de Hon, "Symmetrical pyramidal horn antennas based on EBG structures," *Progress In Electromagnetics Research B*, Vol. 29, 1–22, 2011.
6. Xie, H.-H., Y.-C. Jiao, L.-N. Chen, and F.-S. Zhang, "An effective analysis method for EBG reducing patch antenna coupling," *Progress In Electromagnetics Research Letters*, Vol. 21, 187–193, 2011.
7. Xiao, K., F. Zhao, S. L. Chai, J. J. Mao, and J. L.-W. Li, "Scattering analysis of periodic arrays using combined Cbf/P-FFT method," *Progress In Electromagnetics Research*, Vol. 115, 131–146, 2011.
8. Ren, L.-S., Y.-C. Jiao, J.-J. Zhao, and F. Li, "RCS reduction for a FSS-backed reflectarray using a ring element," *Progress In Electromagnetics Research Letters*, Vol. 26, 115–123, 2011.

9. Mao, Y., B. Chen, H. Q. Liu, J. L. Xia, and J. Z. Tang, "A hybrid implicit-explicit spectral FDTD scheme for oblique incidence problems on periodic structures," *Progress In Electromagnetics Research*, Vol. 128, 153–170, 2012.
10. Veysi, M. and M. Shafaee, "EBG frequency response tuning using an adjustable air-gap," *Progress In Electromagnetics Research Letters*, Vol. 19, 31–39, 2010.
11. Kong, Y. W. and S. T. Chew, "EBG-based dual mode resonator filter," *IEEE Microwave and Wireless Components Letters*, Vol. 14, No. 3, 124–126, Mar. 2004.
12. Coccioli, R., F.-R. Yang, K.-P. Ma, and T. Itoh, "Aperture-coupled patch antenna on uc-pbg substrate," *IEEE Transactions on Microwave Theory and Techniques*, Vol. 47, No. 11, 2123–2130, Nov. 1999.
13. Kim, S.-H., T. T. Nguyen, and J.-H. Jang, "Reflection characteristics of 1-d EBG ground plane and its application to a planar dipole antenna," *Progress In Electromagnetics Research*, Vol. 120, 51–66, 2011.
14. Wang, X., M. Zhang, and S.-J. Wang, "Practicability analysis and application of PBG structures on cylindrical conformal microstrip antenna and array," *Progress In Electromagnetics Research* Vol. 115, 495–507, 2011.
15. Lin, S. Y. and J. G. Fleming, "A three-dimensional optical photonic crystal," *J. Lightwave Technol.*, Vol. 17, 1944–1947, 1999.
16. Wasylkiwskyj, W., "On the transmission coefficient of an infinite grating of parallel perfectly conducting circular cylinders," *IEEE Transactions on Antennas and Propagation*, Vol. 19, No. 5, 704–708, Sep. 1971.
17. Saleh, A. A. M., "An adjustable quasi-optical bandpass filter — Part I: Theory and design formulas," *IEEE Transactions on Microwave Theory and Techniques*, Vol. 22, No. 7, 728–734, Jul. 1974.
18. Kushta, T. and K. Yasumoto, "Electromagnetic scattering from periodic arrays of two circular cylinders per unit cell," *Progress In Electromagnetics Research*, Vol. 29, 69–85, 2000.
19. Pelosi, G., A. Cocchi, and A. Monorchio, "A hybrid FEM-based procedure for the scattering from photonic crystals illuminated by a gaussian beam," *IEEE Transactions on Antennas and Propagation*, Vol. 48, 973–980, Jun. 2000.
20. Yang, H. Y. D., "Finite difference analysis of 2-D photonic crys-

tals," *IEEE Transactions on Microwave Theory and Techniques*, Vol. 44, No. 12, 2688–2695, Dec. 1996.

21. Frezza, F., L. Pajewski, and G. Schettini, "Characterization and design of two-dimensional electromagnetic band-gap structures by use of a full-wave method for diffraction gratings," *IEEE Transactions on Microwave Theory and Techniques*, Vol. 51, No. 3, 941–951, Mar. 2003.
22. Kusiek, A., R. Lech, and J. Mazur, "Analysis of electromagnetic plane wave scattering from 2-D periodic arrangements of posts," *Progress In Electromagnetics Research*, Vol. 129, 69–90, 2012.
23. Jia, H. and K. Yasumoto, "*S*-matrix solution of electromagnetic scattering from periodic arrays of metallic cylinders with arbitrary cross section," *IEEE Antennas and Wireless Propagation Letters*, Vol. 3, No. 1, 41–44, Dec. 2004.
24. Yasumoto, K., H. Toyama, and T. Kushta, "Accurate analysis of two-dimensional electromagnetic scattering from multilayered periodic arrays of circular cylinders using lattice sums technique," *IEEE Transactions on Antennas and Propagation*, Vol. 52, No. 10, 2603–2611, Oct. 2004.
25. Tsang, L., J. A. Kong, and K.-H. Ding, *Scattering of Electromagnetic Waves: Theories and Applications*, John Wiley and Sons, New York, 2000.
26. Yasumoto, K. and K. Yoshitomi, "Efficient calculation of lattice sums for free-space periodic green's function," *IEEE Transactions on Antennas and Propagation*, Vol. 47, No. 6, 1050–1055, Jun. 1999.
27. Harrington, R. F., *Time-harmonic Electromagnetic Fields,* McGraw-Hill Book Company, Inc., New York, 1961.
28. Kusiek, A., R. Lech, and J. Mazur, "A new hybrid method for analysis of scattering from arbitrary configuration of cylindrical objects," *IEEE Transactions on Antennas and Propagation*, Vol 56, No. 6, 1725–1733, Jun. 2008.
29. Kusiek, A. and J. Mazur, "Analysis of scattering from arbitrary configuration of cylindrical objects using hybrid finite-difference mode-matching method," *Progress In Electromagnetics Research*, Vol. 97, 105–127, 2009.
30. Kusiek, A. and J. Mazur, "Application of hybrid finite-difference mode-matching method to analysis of structures loaded with axially-symmetrical posts," *Microwave and Optical Technology Letters*, Vol. 53, No. 1, 189–194, Jan. 2011.